ABAQUS-based hysteresis performance analysis of thorough-diaphragm bolted connection between concrete-filled steel tubular column and steel beam

Houhua Liu [1,#], Junyang Shen [1,#], Peiwen Wang [2,*,#]

[1] Department of Civil Engineering, Southwest Jiaotong University, Chengdu, China, 610097

[2.] Department of Civil Engineering, Liaoning Technical University, Fuxin, China, 123000

* Corresponding Author Email: pawn930@163.com

[#]These authors contributed equally.

Abstract. Concrete-filled steel tube can effectively improve the compressive strength of members, so it is widely used in high-rise buildings, bridges and tunnels. However, there are only limited studies on the hysteresis performance of through-diaphragm plates in steel pipe concrete. In light of the current situation, this paper establishes a model of thorough-diaphragm-diaphragm bolted connection TDBC structure using numerical simulation software ABAQUS, conducting monotonic loading and cyclic displacement loading on it to study the hysteretic performance of this structure. The results reveal that the semi-rigid connection of TDBC contributes to the outwards displacement of the plastic hinge in the beam-column joint, indicating a hysteretic good performance. Furthermore, this study also finds that the flange and web area of steel beams present obvious ductile damage characteristics, which is in line with the design philosophy of strong joints and weak members, reproducing the actual damaging process to a certain extent.

Keywords: Through-diaphragm, Concrete-filled steel tubular column, ABAQUS, Static and cyclic loading, hysteresis performance.

1. Introduction

Concrete-filled steel tube, due to its ability to withstand harsh and extreme environments during construction which can greatly meet the demands of contemporary construction methods, is widely used in high-rise buildings, bridges, and tunnels.

To make the joint of concrete-filled steel tube reasonable structure, convenient in construction, and explicit in force analysis, scholars at home and abroad have proposed numerous improving measures. Zheng et al [1] developed a type of steel pipe concrete column and steel beam joint using through bolts-extended endplate, and researched on the overall deformation, damage morphology, resistance, and strain progress on crucial sections of the joint under continuous collapse. Ye al. [2-3] proposed a vertical through-diaphragm bolted joint between steel pipe concrete column and steel beam, and conducted a physical experiment on loading process, damage mode, and mechanical performance of the joint using the monotonic and cyclic loading method. Zhang et al. [4] carried out cyclic loading experiments on rectangular concrete-filled steel tubular column with steel bar-pierced joint, studying its hysteresis performance, failure mode, energy dissipation and ductility. Sheet et al. [5] experimented on CFT column to steel beam connections under cyclic loading. Cheng et al. [6] proposed a separated internal diaphragm to be used in concrete-filled square steel tubular column and U-shaped steel-concrete composite beam joints, and conducted cyclic loading tests on the joint specimens to evaluate the damage mode, hysteresis performance, ductility, and energy dissipation of each specimen. Ding et al. [7] proposed a CFST column and steel beam joint with bottom-flange-bolted, upper-flange-welded, through-diaphragm, testing its mechanical properties. Azizinamini et al. [8-9] proposed a concrete-filled steel tubular column - steel beam joint with beam penetration, proposed the design method of the joint, and conducted an experimental study on the mechanical properties of the joint.

Although the through-diaphragm steel tubular concrete column and steel beam bolted joint has the advantages of convenient construction, explicit load transferring path and high utilization of space, there are limited studies on this topic. In this paper, with the help of finite element software ABAQUS, a numerical simulation model of steel pipe concrete column and steel beam joint with TDBC is established based on previous research [2-3], researching on its hysteresis performance under monotonic and cyclic loading.

2. Numerical simulation modeling

The numerical simulation model is developed by the finite element software ABAQUS. Each component of the model is created with C3D8R element. Two constitutive models are adopted, with concrete using concrete damage plasticity model [10] and steel using a double broken line model. During the process of meshing, finer meshes are applied to the beam-column joints as well as the sections close to bolts, while the remaining part of the model is reduced to coarse meshes in an attempt to lower the amount of calculation.

2.1. The structure of bolted connection

The beam-column joint section utilizes a vertical through-diaphragm structure, which is illustrated in detail in Fig.1. Two vertical through-diaphragm plates are inserted along the long side of the rectangular-shaped steel tube concrete column. This beam-column joint structure is comprised of steel beams, steel tubular concrete columns, vertical through-diaphragm plates, cover plates, shear plates, and high-strength bolts.

Assembly procedures: Along the long side of the steel pipe column's cross section, vertical through-diaphragm plates penetrate the center of the short side of the steel tubular column and are welded to the steel tubular column. The cover plates are positioned between vertical through-diaphragm plates and steel beams, which are welded both to the vertical through-diaphragm plate and the rectangular steel pipe column. Furthermore, they are also connected to steel beams with M24 high-strength bolts. Shear plates are situated on both sides of the web plates, welded to the steel pipe column, and are connected to the steel beam by means of M20 high-strength bolts.

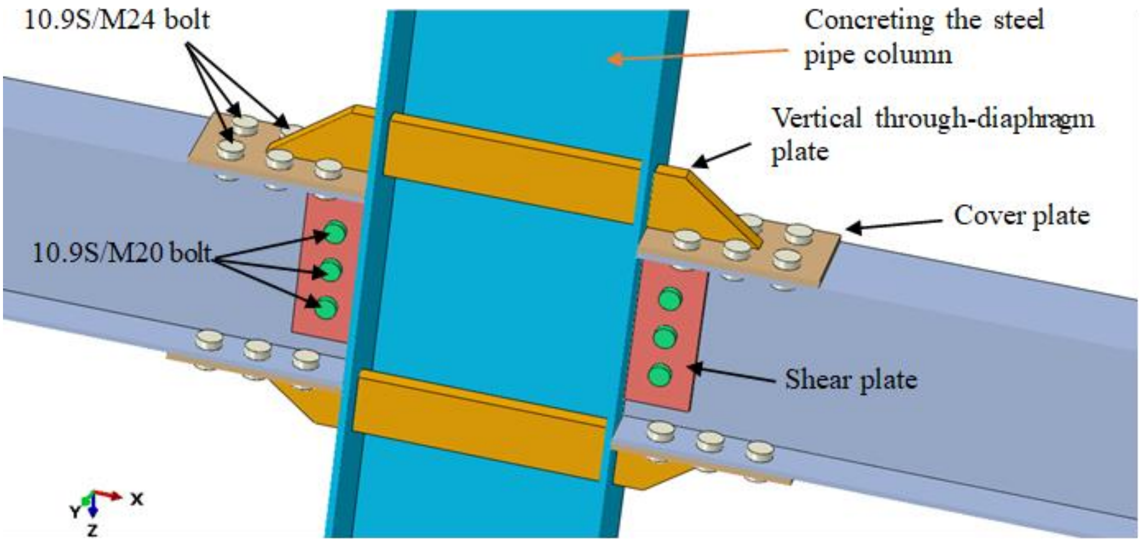

Fig 1. Structure of bolted connection

2.2. Sizes of components and material parameters

The cross section of the steel pipe column is a 440*mm*×220*mm* rectangle, and the steel column measures 2820*mm* in height and 12*mm* in thickness. All steel materials are of the Q345 steel type. The steel beam adopts a cross-sectional size of 170*mm*×350*mm*×6*mm*×10*mm*. What's more, each cover plate is connected by six 10.9-grade M24 high-strength bolts, adding up to a total of 24 bolts

[2-3]. Similarly, each shear plate is linked with three 10.9-grade M20 high-strength bolts, for a grand total of six. To prevent local buckling caused by vertical reciprocating loading in the steel beam, stiffeners are installed on the near-end side of both steel beams by means of welding. The size and material parameters can be found in Table 1 and Fig.2 shows in detail about the plane structure of the model. It is worth mentioning that C40 concrete is poured into the steel tubular columns.

Table 1. Size and material parameters

Component	f_y (MPa)	f_t (MPa)	E (GPa)	ν	B×H×L (mm)
Steel pipe	400	540			220×440×2820
Through-diaphragm	290	440			30×100×540/800
cover plate	415	540			12×170×290
Shear plate	420	540	206	0.28	10×105×260
Stiffener	400	540			10×82×330
Web plate	400	540			6×330×2300
Fringe plate	425	540			10×170×2300

Annotation: B stands for the width of each component’s cross section; H stands for the height of each cross section; L stands for the length of each component.

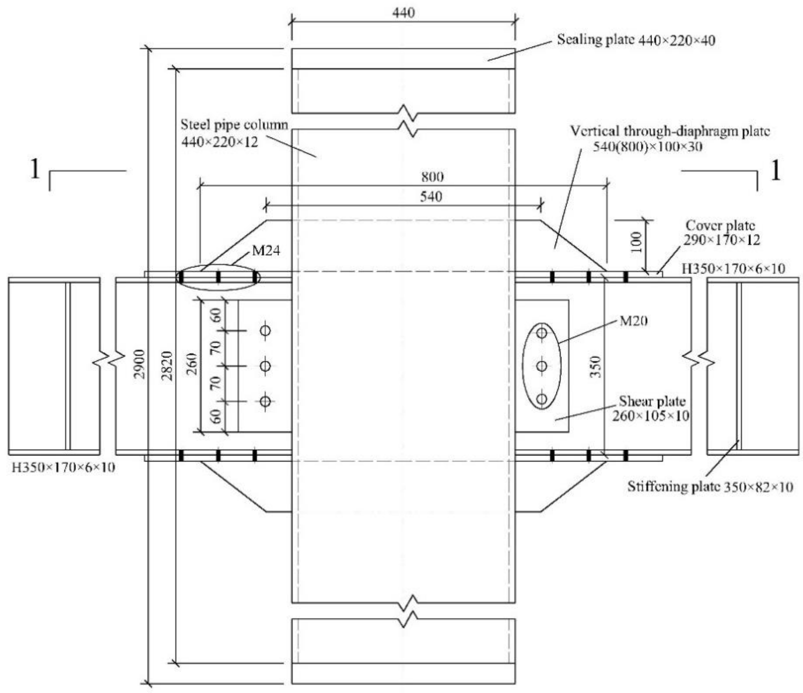

(a)

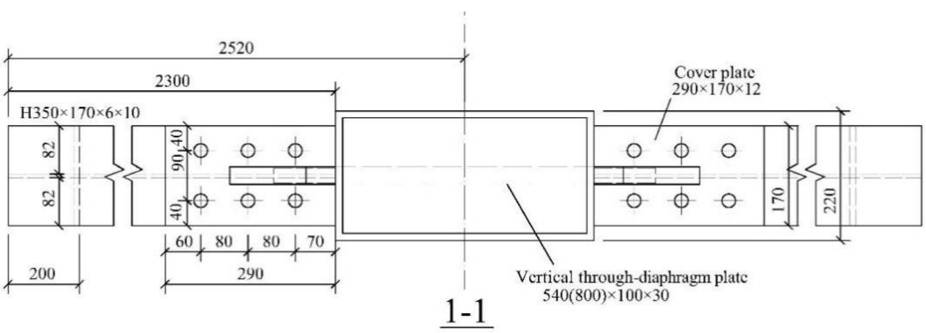

(b)

Fig 2. Size of bolted connection, (a) Plane diagram, (b) Profile diagram.

2.3. Load and constraints

The load in the model consists of vertical axial pressure and vertical displacement stress. The vertical axial force is placed on the center of the steel pipe column's upper cover with an axial compression ratio of 0.3. As to the vertical displacement stress, it's put on the specific point in each steel beam respectively where stiffeners are added. And the initial displacement stress points upward on the starboard beam whereas downward on the left beam. In order to illustrate more plainly about the constraints set on the model, U1, U2, and U3 are used to represent translations along the X, Y, and Z axes, while UR1, UR2, and UR3 indicate rotations around the X, Y, and Z axes, respectively. The cyclic displacement loading mechanism can be noted in Fig.3. Specific constraints and where the load is put on being illustrated in Fig.4.

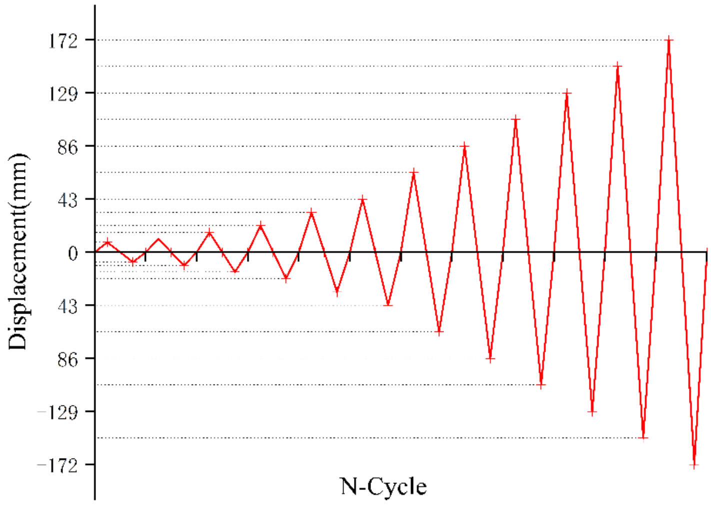

Fig 3. Cyclic loading mechanism

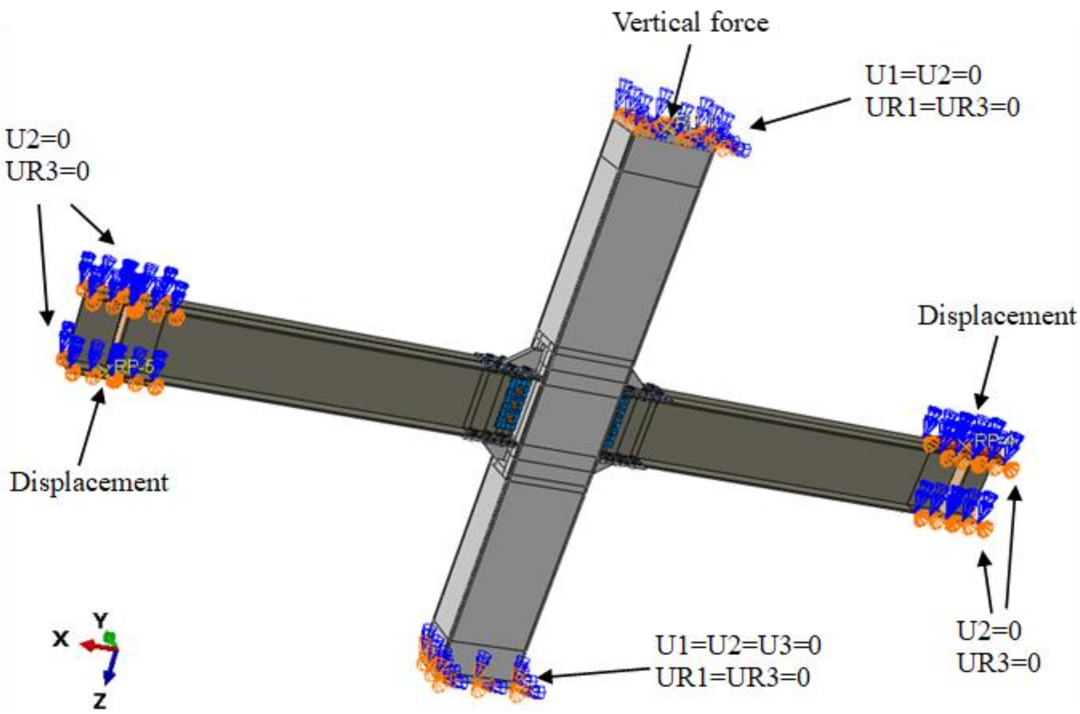

Fig 4. Load and constraints

3. Results

3.1. Strain analysis of TDBC

It can be seen in Fig.5 that on each side of the web plate, three measuring points are designated as F-1-L(R), F-2-L(R), and F-3-L(R) from top to bottom. Meanwhile, another four measuring are fixed on are set on both the upper and bottom flanges. Taking the upper flanges as an example, gauging points are YU(YB)-1-L, YU(YB)-2-L, YU(YB) -1-R, and YU(YB)-2-R respectively. Judging from the outcome, the web plates near the joint where the six measuring points are do not yield until the displacement in the beam end reaches 42*mm*. As soon as the displacement of the beam end reaches 42 *mm*, the gradient of the curves gradually increases, showing signs of yielding. It can also be found that web plates on the compression side enter yielding stage prior to that on the tension side. All the phenomena during this period indicates that the joint enters the elastic-plastic stage. When the displacement reaches 95*mm*, the rate of strain change increases dramatically, meaning that the buckling failure is imminent.

It can also be found that the stiffness of flange plates is inadequate. Flange plate on the left at the bottom (YB-1-L, YB-2-L) reaches yielding stage very early at 28*mm* displacement. Furthermore, an abrupt increase in strain happens to flange plates (YB-1-R, YB-2-R) after they enter yielding stage. Flange plates yield prior to web plates, and the web plates under compression yield faster to web plates under stretch.

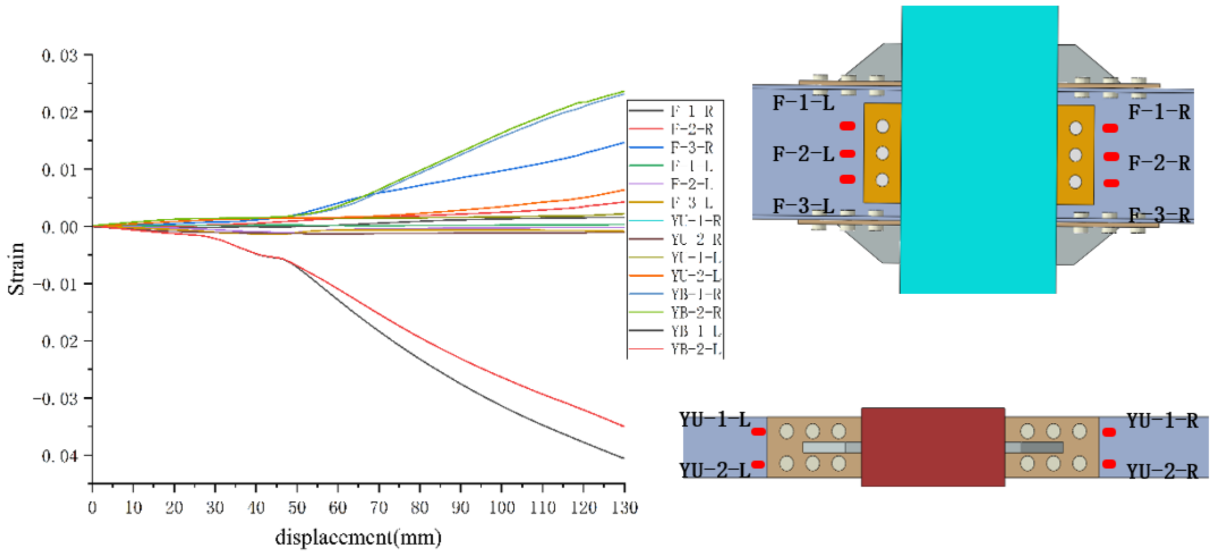

Fig 5. Displacement-Strain Curves

3.2. Hysteresis test results

Considering the efficiency of calculation and accuracy of failure effect under large displacement stress, this paper does not simulate the loading displacement after 107.5*mm* compared to the original field test. As is shown in Fig.6, the typical damage phenomena in cycles of loading displacement of 64.5*mm*, 86*mm*, and 107.5*mm* is recorded. When the loading displacement reaches the first half cycle of 64.5*mm*, rather obvious plastic deformation initially occurs at the outermost bolt connection in the lower flange of the beam on the right. Similarly, when it comes to the second half cycle of 64.5*mm*, obvious plastic deformation also happens to the lower flange of the beam to the left. During the second half cycle of 64.5*mm*, the section between the outermost belt and the second outward bolt in the lower flange of the beam exhibits evident local buckling damage, so does the web plates near the outermost belt. The aforementioned deformation appears half a period later in the beam on the left than that of the right. In the course of the first half cycle of 86*mm* loading displacement, the web plates near the joint produces apparent buckling damage. As the loading displacement enters into its final cycle which is 107.5*mm*, the wall of the outermost bolt hole on the right suffers from a necking fracture due to cumulative tension-compression damage. In the meantime, the flange plates and web plate of the left beam experience severe buckling deformation.

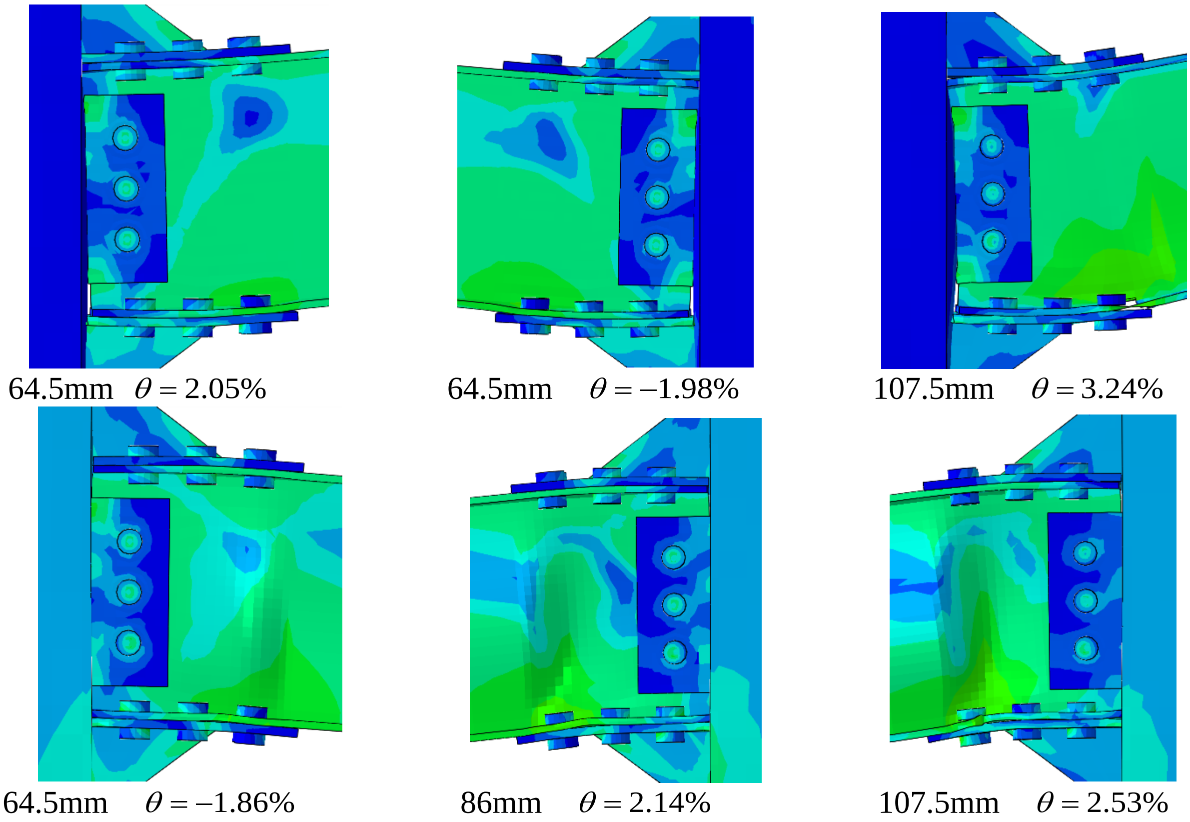

Fig 6. Deformation of the beam-column joint

With its cross section weakened by bolts, the lower flange, which is under the semi-rigid constraint of through-diaphragm plate and bolts, is vulnerable in the face of repeating vertical load. Finally, the equivalent lateral alternating tension-compression load results in the lower flange buckling in its weak areas. Near the beam-column joint, the warping deformation of flange plates induces a gradual increase in the out-of-plane torsion angle of the web plates. When a certain loading displacement is reached, a tiny disturbance exerted on the web plates rapidly cause its overall instability, with some small regions at the root or in the middle of the web plate exhibiting buckling deformation. As the alternating load progresses, the stress level in the joint area increases and gradually enters the plastic stage. Considering the damage accumulation effect of the steel material under cyclic loading, the strength of the joint decreases continuously, and the stiffness continues to degrade until the vulnerable parts of the lower flange where warping deformation first occurs enters failure stage, resulting in necking fracture.

3.3. Hysteresis performance

Fig.7 depicts the hysteresis curve of the through-diaphragm bolted connection simulation test. Overall, the hysteresis curves of the left and right beam are in good agreement with each other. Conforming to the characteristics of bolted connection, both hysteretic curves show continuous progression from elastic to slip, elastic-plastic and finally failure stages. The shape of the hysteresis loop and the moment bearing capacity of each load-displacement stage, within a certain error range, are comparable to physical experiment [2-3]. For instance, the moment bearing capacity within displacement from 86*mm* to 107.5*mm* is concentrated at 210*kN·m*-240*kN·m*, which can recur the mechanical performance and behavioral characteristics of the model in the field test to some extent, close to reality.

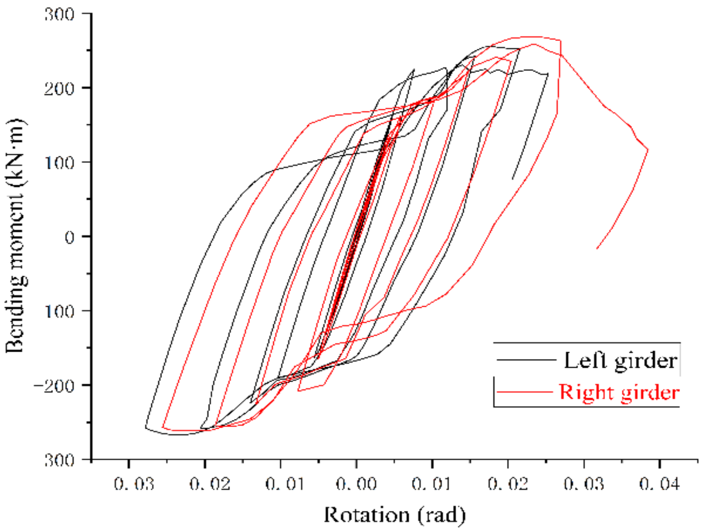

Fig 7. Moment-Rotation Curves

4. Conclusions

Through finite element modeling and the help of ABAQUS, analysis of hysteretic behavior is conducted on through-diaphragm bolted connections between concrete-filled steel column and steel beams, drawing the following conclusions:

(1) TDBC can generate a variable stiffness region near the outermost row of bolts. The assembly of such semi-rigid joints can generate plastic hinges of beam-column joint, and more importantly, moves them outwards from the center of the joint. Beam-column structure installed with TDBC shows excellent hysteresis performance and energy dissipation performance.

(2) The failure phenomenon simulated by finite element model is located in flanges and web plates near the outermost wall of bolt hole, exhibiting characteristics of ductile failure. This kind of failure mode is in line with the design philosophy of strong joints and weak members, and can reproduce the actual damage process to some extent.

References

[1] ZHENG Long, WANG Wenda, LI Huawei, LI Tianhao. Research on performance of CFST column to steel beam joint with through bolts-extended endplate against progressive collapse [J]. Journal of Building Structures, 2019, 40(11):140-149. (in Chinese)

[2] YE Quanxi, WANG Yuanqing, LIN Ying, et al. Analysis of bearing capacity of vertical through diaphragm bolted joint between concrete-filled steel tubular column and steel beam [J]. Journal of Beijing University of Technology, 2021, 47(11):1247-1255. (in Chinese)

[3] YE Quanxi, LI Tongdong, WANG Yuanqing, et al. Analysis of mechanical properties of horizontal through diaphragm bolted joint between concrete-filled steel tubular column and steel beam [J]. Journal of Beijing University of Technology, 2022, 48(05):507-516. (in Chinese)

[4] ZHANG Yanxia, LIU Ziyang, XU Bin, et al. Experimental study on the mechanical property of steel bar-pierced joints of rc beams and rectangular concrete-filled steel tubular columns [J]. Engineering Mechanics, 2022, 39(04):138-150. (in Chinese)

[5] Sheet I S, Gunasekaran U, Macrae G A. Experimental investigation of CFT column to steel beam connections under cyclic loading [J]. Journal of Constructional Steel Research, 2013, 86(86):167-182.

[6] CHENG Rui, ZHANG Jidong, XU Xing, LIU Jichun, PENG Shu. Experimental study on seismic behavior of concrete-filled square steel tubular column to U-shaped steel-concrete composite beam joints with separated internal diaphragm [J/OL]. Journal of Civil and Environmental Engineering, 1-13[2023-04-12]. (in Chinese)

[7] Ding C T, Pan X B, Bai Y, et al. Prefabricated connection for steel beam and concrete-filled steel tube column [J]. Journal of Constructional Steel Research, 2019, 162(11): 1-13.

[8] Elremaily A, Azizinamini A. Experimental behavior of steel beam to CFT column connections [J]. Journal of Constructional Steel Research, 2001, 57(10):1099-1119

[9] Azizinamini A, Shekar Y, Saadeghvaziri M A. Design of through beam connection detail for circular composite columns [J]. Engineering Structures, 1995, 17(3):209-213

[10] GB/T 50010-2010 Code for design of concrete structures. China Building Industry Press, Beijing, 2010.